Zhou et al. *Microsystems & Nanoengineering* (2026)12:144
https://doi.org/10.1038/s41378-026-01281-6

Microsystems & Nanoengineering
www.nature.com/micronano

ARTICLE Open Access

A fully integrated magnetofluidic system enabled by a wax phase barrier for automated multiplex meat adulteration detection

Tianping Zhou[1,2], Changding Li[1,2], Deyong Chen[1,2,3], Junbo Wang[1,2,3]✉ and Nan Li[1]✉

Abstract

Meat adulteration poses serious economic, regulatory, and ethical challenges worldwide, creating an urgent need for rapid, on-site, and multiplex authentication methods. Although polymerase chain reaction (PCR) is the gold standard for nucleic acid analysis, its reliance on laboratory infrastructure and skilled operators limits field deployment, while current isothermal amplification platforms still lack sufficient automation and integration. Here, we present Magtect, a fully automated magnetofluidic system for rapid, multiplex identification of meat adulteration in sheep products. The system integrates magnetic bead–based nucleic acid extraction, ultrasound-assisted washing, magnetic array–guided bead distribution, and parallel multiplex recombinase polymerase amplification (RPA) detection within a single chip. By combining silicone oil with a thermally controllable wax isolation layer, Magtect enables physical spatial separation of multi-step reagents and on-demand mixing during heating, effectively preventing premature reagent contact and cross-interference. Notably, the wax barrier isolates the elution buffer from the RPA master mix, eliminating bead-induced amplification inhibition commonly observed in conventional magnetofluidic designs. Using this platform, adulteration of sheep meat with duck, chicken, or pork components can be fully automatically identified within 30 min. The system achieves a detection limit of 0.1 copies/μL and reliably detects adulteration levels as low as 1%. These results demonstrate that Magtect provides a robust, sensitive, and field-deployable solution for on-site meat authenticity verification, representing a significant step forward in automated food integrity monitoring.

Introduction

Meat adulteration, defined as the fraudulent substitution of high-value meats with lower-cost alternatives, poses a serious global challenge to food safety and market integrity. Since the European horsemeat scandal, this issue has attracted sustained regulatory and public attention[1,2]. In China, mutton—a widely consumed protein source—is frequently adulterated with inexpensive meats such as pork, chicken, or duck[3,4]. These practices not only undermine consumer confidence and cause economic losses, but also introduce potential health risks and violate religious or cultural dietary restrictions[5,6]. Consequently, there is an urgent demand for meat authentication technologies that are rapid, convenient, cost-effective, and suitable for on-site deployment.

Conventional polymerase chain reaction (PCR)–based methods are regarded as the gold standard for meat authentication due to their high sensitivity and specificity[7–9]. However, PCR workflows rely on sophisticated benchtop instruments and trained personnel, confining their use to centralized laboratories and limiting their applicability for point-of-care testing (POCT). Immunoassay-based approaches offer operational simplicity but often suffer from insufficient sensitivity and specificity for reliable species discrimination[10,11]. Isothermal nucleic acid amplification techniques, such as recombinase polymerase amplification (RPA), have emerged as promising alternatives by eliminating thermal cycling and enabling rapid amplification under mild

Correspondence: Junbo Wang (jbwang@mail.ie.ac.cn) or Nan Li (linan2022@aircas.ac.cn)
[1]State Key Laboratory of Transducer Technology, Aerospace Information Research Institute, Chinese Academy of Sciences, Beijing 100190, China
[2]School of Electronic, Electrical and Communication Engineering, University of Chinese Academy of Sciences, Beijing 100049, China
Full list of author information is available at the end of the article

conditions[12–14]. Nevertheless, despite simplifying the amplification step, most RPA-based platforms still involve labor-intensive and complex sample preparation and detection procedures, preventing true workflow simplification and fully automated on-site implementation[15–17].

Microfluidic technology provides a promising route toward integrated nucleic acid testing by enabling miniaturized, fully enclosed systems that reduce contamination risk and facilitate automation[18–20]. In recent years, several microfluidic platforms have been reported for meat adulteration detection. For example, Xiao et al. combined microneedle-based DNA extraction with a handheld centrifugal loop-mediated isothermal amplification (LAMP) chip, achieving detection of 1% adulteration within 60 min[21]. Similarly, a toothpick-based extraction strategy integrated with a centrifugal LAMP device enabled 1% adulteration detection in 40 min[22]. More recently, Xiang et al. developed a centrifugal microfluidic chip integrating microneedle sampling with clustered regularly interspaced short palindromic repeats (CRISPR)–based detection, achieving a detection limit of 0.1% for multiple meat species within 30 min[23]. Despite these advances, most reported platforms omit effective nucleic acid purification and rely on multiple manual operations. Alternatively, some systems retain analytical sensitivity at the cost of workflow simplicity. For instance, Ding et al. reported a centrifugal RPA–CRISPR/Cas12a platform capable of detecting 0.1% adulteration within 1 h[24]; however, this approach required off-chip tube-based nucleic acid extraction, precluding true "sample-to-answer" integration. Collectively, existing microfluidic solutions face a fundamental trade-off between simplified extraction with compromised performance and complex workflows requiring extensive manual intervention, thereby hindering full automation and practical on-site deployment.

Magnetofluidic technology offers a distinctive solution to the integration challenges of on-site nucleic acid testing[25–27]. Unlike conventional microfluidic systems, magnetofluidic platforms manipulate magnetic beads to transport nucleic acids between discrete reagent chambers, enabling integrated enrichment, purification, and elution without complex fluidic control. This bead-mediated transfer inherently isolates amplification reagents from residual meat matrices, thereby improving assay robustness and compatibility with complex food samples. As summarized in Supplementary Table S2, a comparative analysis of major microfluidic paradigms highlights the strengths of magnetofluidics for fully integrated, on-site nucleic acid testing. In particular, magnetofluidic systems enable pump-free operation through magnetic actuation, rely on simplified and compact instrumentation. However, despite these advantages, most reported magnetofluidic systems remain limited in their ability to perform parallel multi-target analysis, a critical requirement for practical on-site meat adulteration detection where multiple potential adulterants must be simultaneously identified. To address this limitation, we previously developed the M-Detector system, which integrates magnetic bead–based nucleic acid extraction, ultrasound-assisted washing, magnetic array–guided bead distribution, and parallel multiplex LAMP within a single chip[28]. This approach enabled scalable multiplex detection in a compact and enclosed format. Nevertheless, a fundamental challenge in magnetofluidic integration remains unresolved. Because magnetofluidic systems rely on immiscible oil phases for reagent separation and lack active fluid pumping, elution is typically achieved by directly introducing magnetic beads into the amplification master mix. This strategy is intrinsically suboptimal, as elution efficiency is limited and, more critically, residual magnetic beads can adsorb and inactivate key enzymes, such as polymerases, leading to compromised amplification efficiency and false-negative results.

In this work, we present Magtect, a fully automated magnetofluidic system for multiplex meat adulteration detection, applied to the identification of sheep, pork, chicken, and duck DNA. A central innovation of Magtect is the introduction of a wax isolation layer within the amplification chamber. Using a highly versatile centrifugation-based fabrication method, a dense solid wax barrier is formed to physically separate the elution buffer from preloaded RPA reagents. This design ensures that magnetic beads used during extraction and washing are never introduced into the amplification reagents, thereby completely eliminating bead-induced inhibition. Upon heating, the wax layer melts in a controlled manner, allowing the eluted nucleic acids to mix with the underlying RPA reagents and initiate amplification. Furthermore, we systematically investigate the scalability and design constraints of the chip by analyzing magnetic bead resuspension, aggregation, and transfer behaviors across chambers with varying diameters. These results establish practical guidelines for chip scaling and multiplex expansion. Overall, Magtect system achieves full automation from nucleic acid extraction to parallel multiplex RPA detection, providing a rapid and reliable platform for on-site meat authenticity verification.

Results and discussion

Magtect system operation workflow

The Magtect system comprises a disposable Magtect chip and a portable control analyzer, enabling fully automated magnetic bead–based nucleic acid extraction and multiplex RPA detection. The analyzer integrates motion control, magnetic manipulation, ultrasonic actuation, temperature regulation, and optical signal

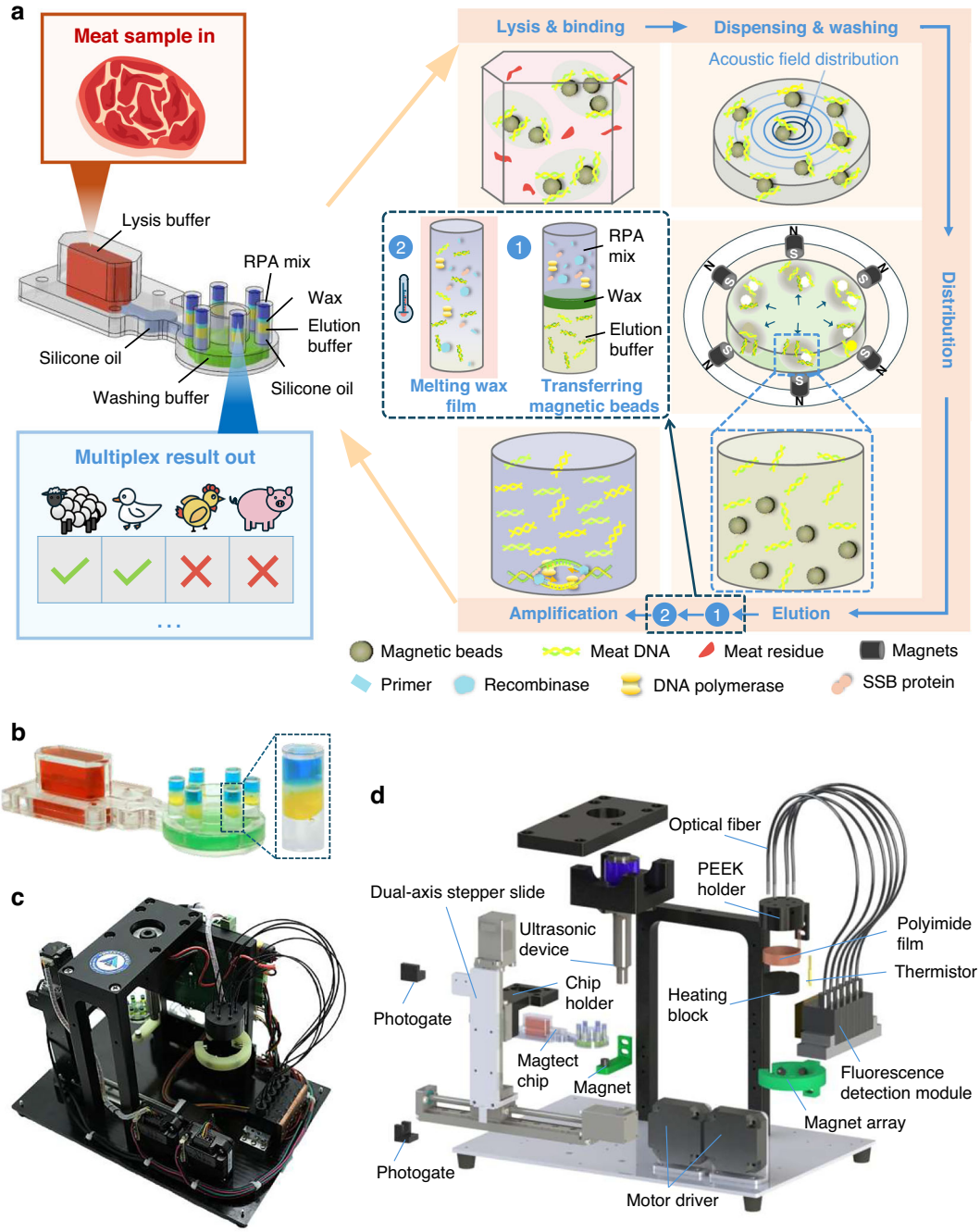

Fig. 1 . Overview of the Magtect system for multiplex meat authentication. **a** Schematic of the fully integrated "sample-to-answer" workflow, showing on-chip magnetic bead–based nucleic acid extraction, ultrasound-assisted washing, magnetic array–guided bead distribution, and parallel isothermal amplification. The centrifugally formed wax barrier is highlighted, which physically isolates the elution buffer from the amplification reagents and melts upon heating to trigger the reaction. **b** Photograph of the assembled Magtect chip. **c** Photograph of the portable Magtect analyzer. **d** Exploded view of the analyzer, illustrating the integrated motion control, magnetic manipulation, ultrasonic washing, heating, optical detection modules

acquisition, allowing all assay steps to be executed in a closed and hands-free manner. The complete operation workflow of the Magtect system is illustrated in Fig. 1a and Fig. S12 and consists of four sequential steps: sample lysis, magnetic bead washing, compartmentalized elution, and multiplex amplification detection.

Step 1: Sample lysis and magnetic bead capture. After sample lysis, the analyzer actuates the vertical stepper

motor to position the Magtect chip adjacent to a fixed magnet, enabling efficient capture of magnetic beads at the bottom of the lysis chamber. The chip is then translated horizontally, transferring the bead aggregate through the silicone oil–filled transfer channel toward the downstream washing zone.

Step 2: Magnetic bead washing via ultrasonic dispersion. The Magtect chip is aligned with the integrated ultrasonic transducer. Upon activation, the ultrasonic field uniformly disperses the magnetic beads within the washing buffer, ensuring thorough resuspension and effective removal of residual inhibitors from the meat matrix.

Step 3: Compartmentalized elution through magnetic redistribution. The chip is positioned within an annular magnet array, where the spatially uniform magnetic field redistributes the dispersed beads into six discrete clusters, each aligned with an individual reaction chamber. The chip is subsequently lowered vertically, guiding each bead cluster through the silicone oil interface into its designated elution zone. During this process, the beads remain physically separated from the underlying RPA reagents by a solid wax barrier, enabling compartmentalized nucleic acid elution without bead–reagent contact.

Step 4: Multiplex amplification detection initiated by wax melting. After elution is completed, the Magtect chip is raised to retrieve the magnetic beads back into the washing zone. The chip is then transferred to the heating module, where controlled heating melts the wax barrier, allowing the elution buffer containing target nucleic acids to merge with the preloaded RPA reagents. Isothermal amplification is subsequently performed at the preset temperature. Real-time fluorescence signals from all six reaction chambers are continuously acquired by the optical detection module and wirelessly transmitted to the companion mobile application.

Ultrasonic and magnetic field optimization for scalable chip design

Multiplex detection in the Magtect magnetofluidic system relies on two sequential and interdependent physical processes: uniform dispersion of aggregated magnetic beads by an ultrasonic field, followed by controlled redistribution of the beads into discrete clusters using a spatially uniform magnetic field. To systematically define the optimal operating conditions for these processes and to establish design guidelines for scalable Magtect chip development, ultrasonic and magnetic field parameters are evaluated through a combination of numerical simulations and experimental validation.

Ultrasonic mixing is first examined, as complete bead resuspension is a prerequisite for uniform downstream magnetic redistribution. COMSOL simulations are performed to analyze the acoustic pressure distribution under constant power conditions. The results show that the central acoustic pressure profile remains stable, while increasing chamber diameter extends the peripheral region into the acoustic attenuation zone, leading to a pronounced pressure drop at the chamber edge (Supplementary Fig. S6). This effect suggests that beads located near the periphery may experience delayed or incomplete resuspension as chamber size increases. Experimental measurements confirm these predictions. For chamber diameters ranging from 13 to 23 mm, complete bead resuspension is achieved, with resuspension time increasing proportionally with diameter. Grayscale-based image analysis further shows that the grayscale ranges of all selected regions remain below the threshold value of 20, indicating uniform bead dispersion. In contrast, when the diameter is expanded to 25 and 27 mm, the effective acoustic field (defined as coverage ≥25 dB) no longer fully spans the chamber, resulting in bead accumulation at the edges and incomplete resuspension, where multiple regions exhibit grayscale differences far exceeding the threshold, revealing pronounced bead aggregation. (Fig. 2a, Supplementary Fig. S7 and Fig. S15). These results identify ultrasonic mixing, rather than magnetic manipulation, as the primary factor determining the upper limit of chip scalability in the present system.

Within the acoustically viable design space (≤23 mm chamber diameter), magnetic field configurations are subsequently optimized to enable uniform bead aggregation and transfer. Circular magnet arrays composed of multiple individual permanent magnets are evaluated, where the diameter of each single magnet is varied from 3 to 8 mm to balance magnetic performance and system miniaturization. COMSOL simulations using the Magnetic Fields, No Currents model are performed to compare magnetic field intensity and lateral coverage generated by arrays assembled from individual magnets of different diameters (Fig. 2b and Supplementary Fig. S8). Experimental validation is conducted by ultrasonically dispersing magnetic beads in wash buffer, followed by magnetic collection using each circular array. The resulting aggregation patterns and time-dependent behaviors are systematically analyzed (Fig. 2b, Supplementary Fig. S9 and Supplementary Fig. S16). Individual magnets with diameters of 3 and 4 mm generate sufficient magnetic force but provide limited lateral coverage when assembled into an array, resulting in incomplete aggregation with low grayscale values and reduced coverage ratios indicating pronounced residual bead accumulation and central clustering. Arrays composed of 5 and 6 mm individual magnets exhibit similar field distributions and reach aggregation saturation within approximately 8 s, with comparable grayscale values indicating similar levels of residual beads. Although arrays constructed from 8 mm magnets minimize residual beads with the highest coverage and grayscale values, their excessively broad

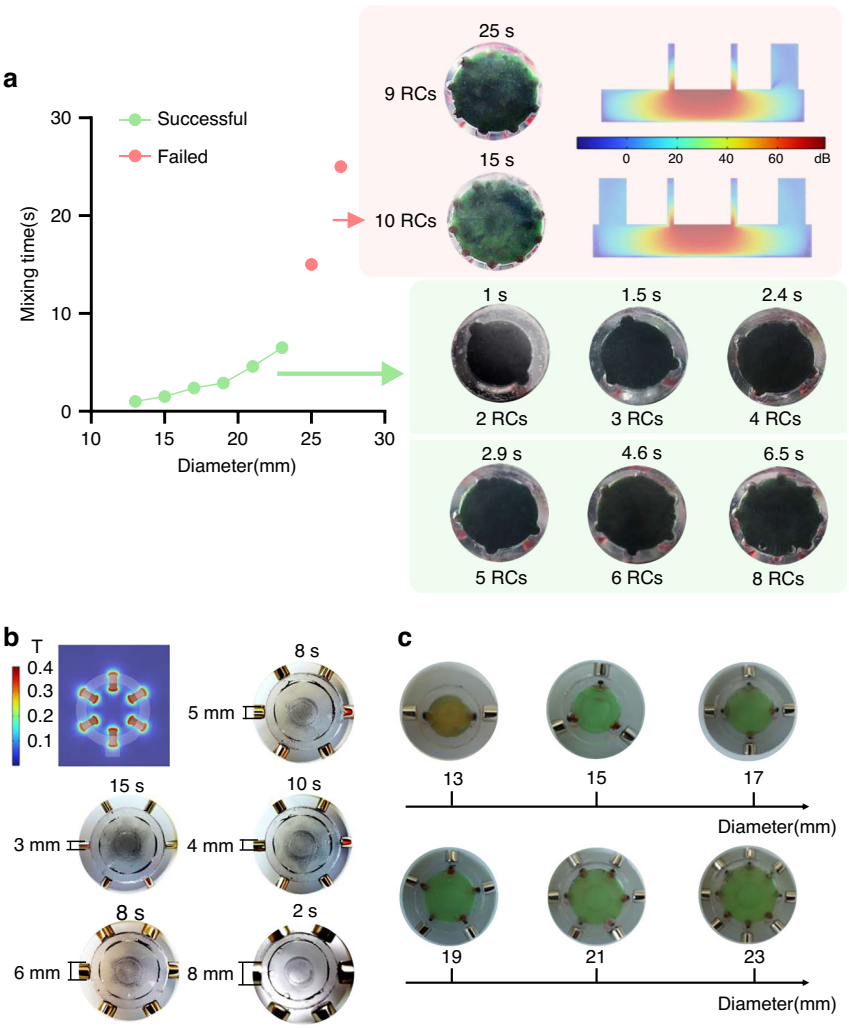

Fig. 2 . Simulation and experimental validation of ultrasonic and magnetic field optimization for scalable chip design. **a** Bead resuspension times in chips with different chamber diameters, including stable-time outcomes for 2–8 chamber chips with complete resuspension, 9–10 chamber chips exhibiting bead accumulation, and corresponding COMSOL simulation results. **b** Simulated magnetic field distributions of individual magnets with diameters of 3, 4, 5, 6, and 8 mm within the array, together with experimental observations of magnetic bead aggregation at the stable time point. **c** Experimental validation of magnetic bead aggregation behavior in 2–8 chamber chips with chamber diameters ranging from 13 to 23 mm under the optimized 5 mm magnet array. RCs represent for reaction chambers

magnetic fields produce overlapping attraction zones that may compromise controlled bead partitioning between adjacent chambers. Considering aggregation efficiency, field confinement, and compatibility with dense chamber layouts, the circular array composed of 5 mm individual magnets is selected as the optimal configuration.

Magnetic bead aggregation and transfer are then evaluated using the selected 5 mm magnet array across the ultrasonically defined chamber size range. For chamber diameters up to 23 mm, beads are consistently aggregated into well-defined clusters and efficiently transferred into the downstream reaction chambers (Fig. 2c and Supplementary Fig. S10). These results demonstrate that, once complete ultrasonic resuspension is ensured, the optimized magnetic field provides sufficient force density for robust and reproducible bead manipulation.

Overall, effective multiplex bead handling in the Magtect system is governed by two sequential criteria. First, an adequate ultrasonic pressure field must be established to achieve complete bead resuspension, which defines the maximum operable chamber size. Second, within this constraint, an appropriately sized magnet array must be selected to enable uniform bead aggregation and transfer. As the detection chambers are arranged circumferentially above the washing chamber, increasing multiplexing requires either larger chamber diameters with higher ultrasonic power and cost, or denser chamber layouts with increased fabrication complexity. These approaches

involve inherent trade-offs between throughput, system cost, and manufacturability. Based on these considerations, a Magtect chip incorporating six reaction chambers with a diameter of 19 mm is adopted for subsequent experiments, providing an optimal balance between acoustic performance, magnetic efficiency, and device compactness.

Development and optimization of a wax barrier for Magtect chip

Conventional magnetofluidic systems rely on oil-phase isolation to separate reagents and lack active fluid-mixing mechanisms. Consequently, nucleic acids captured on magnetic beads are typically eluted directly into the amplification master mix, which restricts the choice of compatible amplification chemistries. In particular, RPA reagents exhibit poor compatibility with bead-based elution. In our preliminary tests, direct elution of nucleic acids from magnetic beads into the RPA master mix led to severe inhibition and frequent amplification failure (Supplementary Fig. S11). This limitation highlights a fundamental bottleneck of conventional magnetofluidic designs and motivates the development of a more flexible strategy to decouple bead elution from amplification.

To overcome this limitation within a static chip architecture, we introduce a temperature-responsive wax barrier that physically separates the elution buffer from the amplification reagents and enables their controlled mixing by thermal actuation. During chip preparation, RPA reagents are first dispensed into each reaction chamber, followed by overlaying molten wax preheated to 48 °C. To form a dense and uniform wax membrane, the chip is placed in a custom-designed holder that constrains its orientation and ensures that the centrifugal force is applied perpendicular to the plane of the reaction chambers. Centrifugation at 3000 rpm for 5 min drives the molten wax to spread evenly and compactly across the chamber cross-section (Fig. 3a). Upon cooling, the wax solidifies into a continuous barrier that effectively isolates the amplification reagents from the upper fluidic layers. Subsequently, the elution buffer and a silicone oil layer are sequentially added above the wax, establishing a vertically stratified structure.

During operation, magnetic beads carrying purified nucleic acids are transported into the elution buffer located above the wax barrier, where elution occurs without direct exposure of the amplification reagents to the beads. After elution, the beads are magnetically removed. The chip is then transferred to a heating module, where controlled heating melts the wax barrier, allowing the eluate to merge with the pre-stored RPA reagents and initiate isothermal amplification in the absence of bead-induced inhibition.

The volume of wax is first optimized to ensure reliable physical separation while minimizing reagent consumption. A wax volume of 3 μL is insufficient to form a continuous membrane and frequently results in incomplete coverage or adhesion to the chip sidewalls, leading to unintended mixing. Volumes of 5 μL or greater consistently generate visually intact barriers; however, functional testing reveals that barriers formed with 5 μL occasionally rupture under ultrasonic agitation used in the chip workflow. In contrast, barriers formed with 7 μL and 9 μL remain structurally intact after ultrasonic treatment (Fig. 3b). Considering robustness and volume efficiency, 7 μL is selected as the optimal wax volume for subsequent experiments.

Next, the thermal conditions required for efficient wax melting and reagent mixing are systematically investigated. Given the melting point of the wax (~40 °C), the minimum heating time required for barrier removal is evaluated at 42, 44, 46, 48, and 50 °C using dye-labeled solutions to visualize mixing. The onset of visible mixing occurs at 90, 60, 60, 30, and 30 s, respectively (Fig. 3c). These conditions are then applied as pre-heating steps prior to standard RPA incubation at 40 °C to assess their impact on amplification performance. Heating at 42 °C and 44 °C yields high and comparable amplification efficiencies, whereas higher pre-heating temperatures (≥46 °C) result in progressively reduced performance, with complete amplification failure observed after pre-heating at 50 °C (30 s) (Fig. 3d).

To balance rapid barrier removal with preservation of amplification activity, a pre-heating condition of 44 °C for 60 s is selected as optimal. Under this condition, the wax melts efficiently and remains in a liquid state during subsequent incubation at 40 °C. Owing to its lower density, the molten wax migrates upward, passively promoting mixing between the eluate and the underlying RPA reagents. In contrast, higher pre-heating temperatures likely compromise temperature-sensitive RPA components, leading to reduced amplification efficiency. Collectively, this optimized wax-mediated strategy enables robust decoupling of bead-based elution and sensitive amplification chemistries within an integrated magnetofluidic chip.

Optimization of on-chip nucleic acid extraction parameters

To obtain efficient and reproducible characteristic of the integrated magnetofluidic system, four significant parameters governing on-chip nucleic acid extraction were systematically optimized: lysis/binding time, magnetic bead volume, washing time, and elution time. All experiments were conducted using a quantified sheep meat homogenate (1 copy μL^{-1}) as the model sample. Extracted nucleic acids were analyzed directly on-chip, with all six reaction chambers preloaded with sheep-

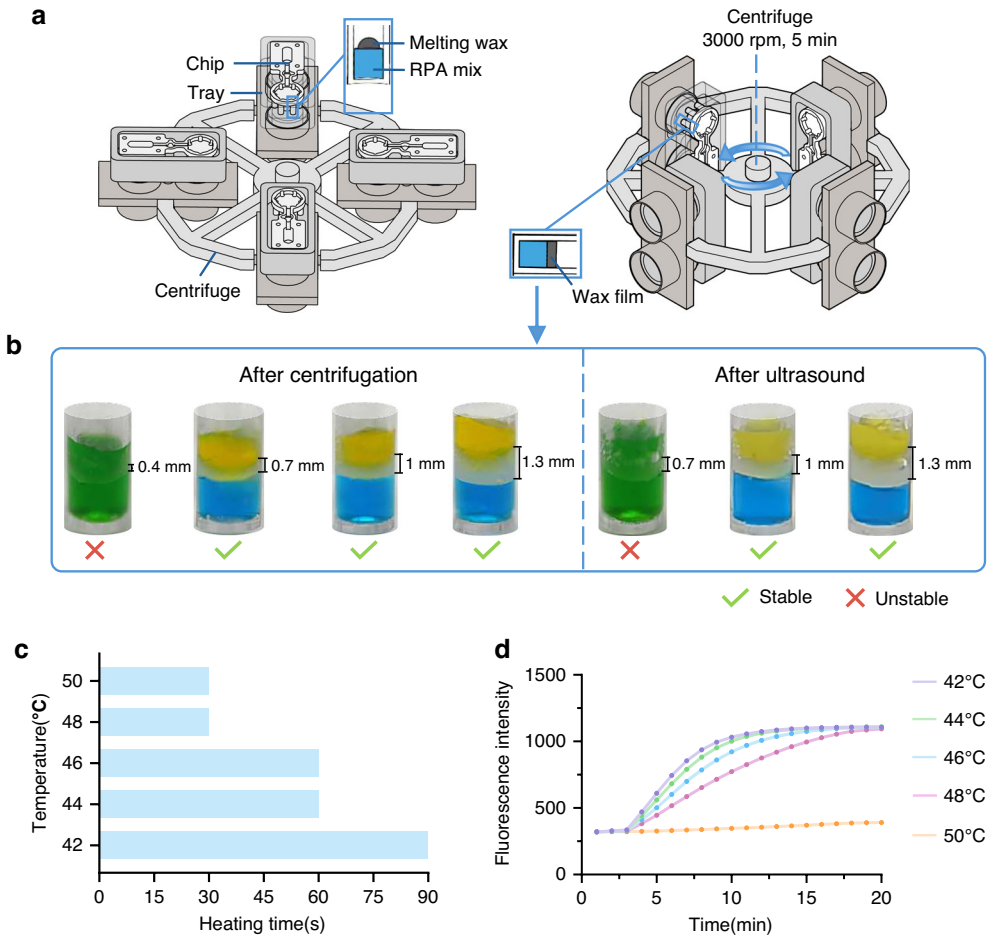

Fig. 3 . Preparation and optimization of the wax isolation layer. **a** Formation of the wax layer in reaction chambers via centrifugation at 3000 rpm for 5 min. **b** Optimization of wax layer thickness using wax volumes of 3, 5, 7, and 9 µL, corresponding to layer thicknesses of 0.4, 0.7, 1.0, and 1.3 mm, respectively. A 0.4 mm layer failed to support the elution buffer, while the 0.7 mm layer was disrupted under ultrasonic conditions. **c** Melting time of a 1.0 mm wax layer at different heating temperatures. **d** Effect of heating temperature on amplification activity

specific RPA reagents. Extraction efficiency under each condition was evaluated based on real-time amplification kinetics, with the earliest amplification onset used as the primary optimization criterion. All experiments were performed in triplicate to ensure reproducibility.

Lysis/binding times of 2.5, 5, 7.5, and 10 min were evaluated while keeping the magnetic bead volume (20 µL), washing time (15 s), and elution time (5 min) constant. As shown in Fig. 4a, increasing the lysis time progressively advanced the amplification onset up to 7.5 min, indicating improved nucleic acid release and binding efficiency. Further extension to 10 min did not result in an earlier signal rise. Therefore, 7.5 min was selected as the optimal lysis/binding time, balancing extraction efficiency and total assay duration.

Magnetic bead volumes of 10, 20, 40, and 80 µL were tested under the optimized lysis condition (7.5 min), with washing and elution times fixed at 15 s and 5 min, respectively. As illustrated in Fig. 4b, 10 µL of beads resulted in delayed amplification onset and occasional reaction failure, likely due to insufficient bead recovery and transfer. In contrast, bead volumes of 20 µL and above produced similarly early amplification onsets, with no further improvement observed at higher volumes. Accordingly, 20 µL was selected as the optimal bead volume.

Washing times of 15, 30, 45, and 60 s were evaluated using the optimized lysis time and bead volume, with a fixed elution time of 5 min. As shown in Fig. 4c, variations in washing duration did not noticeably affect the timing of amplification onset, suggesting that ultrasonic agitation ensured effective impurity removal even with a brief wash. Consequently, a washing time of 15 s was adopted.

Elution times of 1, 3, 5, and 7 min were investigated with all other parameters set to their optimized values. As shown in Fig. 4d, extending the elution time from 1 to 3 min significantly advanced the amplification onset,

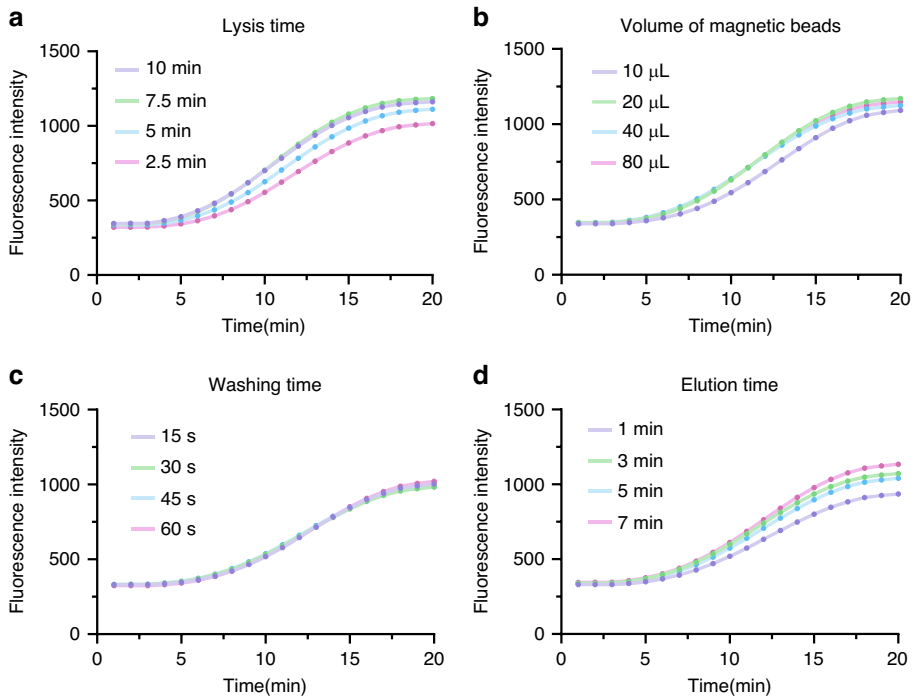

Fig. 4 . Optimization of key on-chip nucleic acid extraction parameters. Real-time amplification curves used to determine the optimal conditions for **a** lysis/binding time, **b** magnetic bead volume, **c** washing time, and **d** elution time. Quantified sheep meat homogenate was used as the model sample. Curves represent the mean values of triplicate experiments, and the earliest and steepest amplification onset was used as the criterion for optimal extraction efficiency

reflecting more efficient nucleic acid release from the beads. Longer elution times did not further accelerate signal initiation. Therefore, 3 min was identified as the optimal elution duration.

In conclusion, the optimized on-chip nucleic acid extraction protocol consisted of 7.5 min lysis/binding, 20 μL magnetic beads, 15 s washing, and 3 min elution. This configuration enables rapid amplification initiation while maintaining robust compatibility with downstream on-chip RPA, supporting sensitive and reliable multiplex meat species detection.

Specificity and sensitivity validation

The analytical specificity and sensitivity of the Magtect system were evaluated using quantified liquid homogenates (1 copy μL^{-1}) of sheep, pork, chicken, and duck as model samples. For each chip run, a positive control containing a mixture of all four target DNAs and a negative control consisting of nuclease-free water were included to verify assay reliability.

Specificity was assessed by preloading species-specific RPA reagents into individual reaction chambers. Each single-species homogenate was processed independently on separate chips, with experiments performed in triplicate. As shown in Fig. 5a–d, amplification signals were exclusively observed in reaction chambers containing the corresponding primer sets, with no detectable cross-reactivity across non-target chambers. This absence of cross-talk is ensured by the fully enclosed design of each reaction chamber together with the spatial isolation inherent to the chip architecture, which effectively suppresses both fluidic cross-contamination and optical signal leakage between adjacent chambers (Supplementary Fig. S14). These results confirm the high primer specificity as well as the effectiveness of the enclosed magnetofluidic architecture in preventing cross-contamination.

Sensitivity was evaluated using serial tenfold dilutions of each meat homogenate, ranging from 10 to 0.01 copies μL^{-1}, with three replicates per concentration. As shown in Fig. 5e–h, the Magtect system consistently detected all four target species down to 0.1 copy μL^{-1}, demonstrating uniform and high analytical sensitivity across all reaction chambers.

Collectively, these results demonstrate that the Magtect system delivers robust species specificity and high sensitivity within a fully integrated magnetofluidic platform, supporting its suitability for reliable, multiplex meat authentication in POCT applications.

Validation with simulated meat adulteration samples

To assess the performance of the Magtect system under realistic adulteration scenarios, simulated meat mixtures were prepared by blending sheep meat with a common

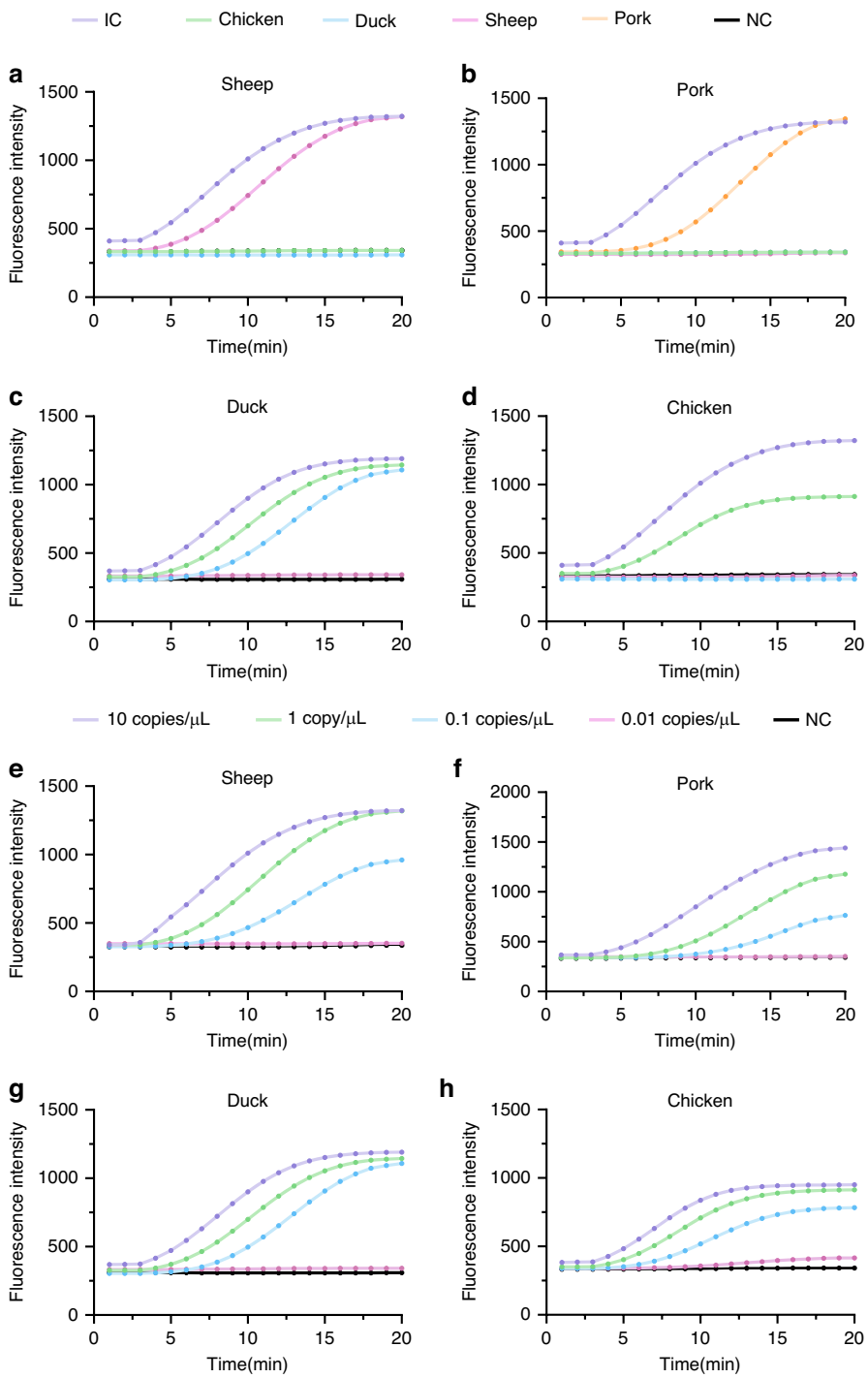

Fig. 5 . Specificity and sensitivity validation of the Magtect system. Specificity evaluation for **a** sheep, **b** pork, **c** duck, and **d** chicken targets. Amplification signals were observed exclusively in reaction chambers containing the corresponding species-specific primer sets when tested with individual DNA samples, demonstrating high specificity without cross-reactivity. Sensitivity evaluation for **e** sheep, **f** pork, **g** duck, and **h** chicken targets. Serial tenfold dilutions of meat homogenates (10 to 0.01 copies/μL) were tested. The system consistently detected each target down to 0.1 copies/μL, as indicated by distinct amplification curves. All curves represent the mean values of triplicate experiments

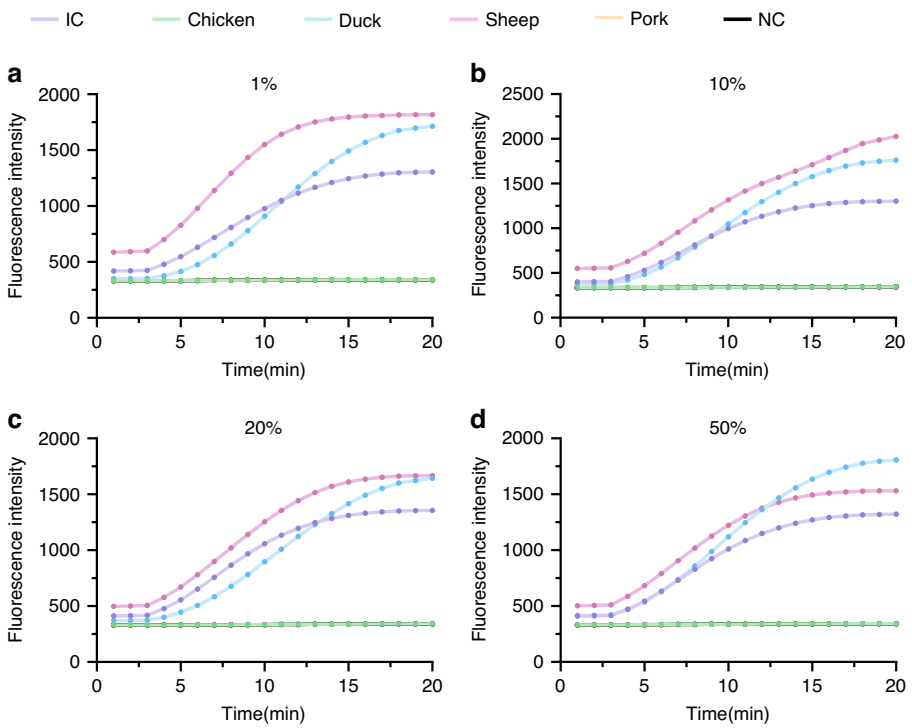

Fig. 6 . On-chip detection of simulated meat adulteration. Detection results for sheep meat adulterated with duck meat at ratios of **a** 1%, **b** 10%, **c** 20%, and **d** 50% (w/w). Both sheep- and duck-derived DNA were successfully identified across all tested adulteration levels, demonstrating the capability of the Magtect system for multiplex on-chip authentication

adulterant, duck meat. Homogeneous minced samples were generated at defined weight/weight (w/w) ratios of 1%, 10%, 20%, and 50% using a mechanical grinder, corresponding to sheep-to-duck mass ratios of 9.9:0.1 g, 9:1 g, 8:2 g, and 5:5 g, respectively (Supplementary Fig. S13). For on-chip analysis, approximately 1 g of each blended sample was introduced into the lysis zone of the Magtect chip.

All samples were analyzed in triplicate under optimized assay conditions. As shown in Fig. 6a–d, the system consistently detected both sheep- and duck-derived DNA across the full range of adulteration levels tested. Distinct amplification signals were observed in the corresponding reaction chambers preloaded with sheep- and duck-specific RPA reagents, respectively. Notably, reliable detection was achieved even at the 1% adulteration level, demonstrating sensitivity compatible with regulatory requirements for identifying economically motivated meat adulteration. These results confirm that the Magtect system enables accurate and automated detection of low-level meat adulteration within a fully integrated magnetofluidic workflow, highlighting its potential for practical on-site food authenticity verification.

Conclusion

In this work, we present Magtect, a fully automated magnetofluidic system designed for rapid, on-site multiplex authentication of meat species. The system achieves sensitive and specific identification of sheep, pork, chicken, and duck DNA, with a detection limit of 0.1 copy/μL—corresponding to 1% adulteration—within 30 min. This performance meets practical requirements for field-deployable meat authenticity testing and demonstrates the feasibility of integrating complex nucleic acid workflows into a compact, user-friendly platform.

Compared with existing magnetofluidic approaches, Magtect integrates all essential sample-to-answer operations within a single chip. Its central innovation is the introduction of a centrifugally cast, temperature-responsive wax barrier that physically separates the elution buffer from preloaded RPA reagents. This design resolves a fundamental limitation of conventional pump-free magnetofluidics, where the absence of active fluid mixing typically requires direct elution of nucleic acids together with magnetic beads into the amplification mixture. By preventing magnetic beads from entering the amplification phase, the wax barrier eliminates bead-induced inhibition and enables robust integration of bead-based extraction with sensitive RPA chemistry within a static fluidic architecture. As a result, elution and amplification are effectively decoupled, substantially broadening the assay compatibility of magnetofluidic systems

for POCT. Moreover, the optimized low-temperature melting protocol ensures rapid and well-controlled barrier removal without compromising amplification efficiency, further supporting reliable and fully automated multiplex detection. The system-level design is further strengthened by systematic optimization of ultrasonic and magnetic field parameters, which establishes clear physical constraints for scalable chip design. Uniform bead resuspension enabled by ultrasound, followed by deterministic bead partitioning under a spatially uniform magnetic field, forms the basis for robust multiplex detection. These design principles provide practical guidelines for adapting the Magtect platform to different levels of multiplexing and assay requirements. Beyond meat authentication, the Magtect platform is inherently adaptable to a broad range of nucleic acid testing applications that employ magnetic bead–based extraction and isothermal amplification. Consequently, other applications employing similar biochemical strategies—such as multiplex clinical diagnostics for respiratory or sexually transmitted pathogens, or environmental monitoring of waterborne microorganisms—can be accommodated with minimal system modification. In most cases, adaptation primarily involves the design of target-specific primers and probes, together with optimization of the lysis buffer for the corresponding sample matrix. One limitation is that applications involving extremely dilute samples may require additional upstream concentration, as the fixed on-chip lysis volume can constrain the achievable absolute sensitivity.

Despite these advantages, the current system has limitations. The use of a wax barrier, while effective and robust, introduces an additional fabrication step during chip preparation. In addition, although Magtect supports multiplex target detection within a single run, overall throughput is currently limited to one sample per chip. Scaling to higher multiplexing levels can be realized by increasing ultrasonic power or adopting spatially distributed ultrasonic transducers to support bead dispersion in larger chamber arrays, in combination with a greater number of circumferential magnets. However, increasing the number of reaction chambers inevitably divides a finite bead population into smaller fractions, reducing the nucleic acid input per chamber and potentially lowering detection sensitivity. Practical system design, therefore, requires a balance between multiplexing capacity and analytical sensitivity. Additional strategies, such as upstream pre-amplification or multicolor fluorescence detection, may further extend multiplexing capability without a proportional increase in cartridge footprint.

In conclusion, this study demonstrates a fully integrated, automated magnetofluidic platform capable of true “sample-in–result-out” detection for meat adulteration. By introducing a simple yet robust wax-based phase separation strategy, Magtect overcomes a long-standing bottleneck in magnetofluidic integration and improves compatibility with sensitive amplification chemistries. These advances position Magtect as a practical and scalable solution for on-site food authenticity monitoring and broader molecular diagnostics.

Materials and methods

Reagents and materials

Reagents for magnetic bead–based nucleic acid extraction, including lysis/binding buffer, washing buffer, and magnetic beads, were obtained from Magen Biotechnology (IVD5412, Guangzhou, China). RPA kits for sheep (KM105), pork (KM106), chicken (KM101), and duck (KM102) were purchased from XianDa Gene Technology (Suzhou, China). Quantitative PCR (qPCR) master mix was purchased from TransGen Biotech (AQ711, Beijing, China). Primer and probe sequences used for qPCR validation are listed in Table S1. Silicone oil was purchased from Dow Corning (DC184, Michigan). Wax with a melting point of approximately 40 °C was custom manufactured by Hushi Laboratory Equipment (Shanghai, China).

Design and fabrication of the Magtect chip

The Magtect chip was designed using SolidWorks (Dassault Systèmes) and fabricated from polycarbonate. The chip dimensions were 72 mm × 25 mm × 14 mm (length × width × height). The chip integrates four functional zones: a lysis zone, a transfer zone, a washing zone, and six circumferentially arranged reaction chambers (Fig. 1b and Supplementary Fig. S1).

The lysis zone accommodates sample loading, tissue lysis, and initial nucleic acid capture by magnetic beads. A silicone oil–filled transfer zone connects the lysis and washing zones, enabling bead transport while preventing liquid mixing. The washing zone contains an ultrasonically compatible cavity for bead resuspension and impurity removal. Each reaction chamber is vertically stratified, consisting (from bottom to top) of preloaded RPA reagents, a solidified wax barrier, an elution buffer layer, and a silicone oil overlayer. The wax barrier physically separates elution and amplification reagents and enables controlled mixing upon heating. Wax barriers were formed by dispensing molten wax into the reaction chambers, followed by centrifugation at 3000 rpm for 5 min using a benchtop centrifuge (L530R, Cence Laboratory Instrument Development, Changsha, China). After solidification, the silicone oil layer isolated the reaction chambers from the washing zone, minimizing evaporation and cross-contamination. The chip was sealed with a laser-cut polymethyl methacrylate (PMMA) lid using double-sided adhesive tape (9472LE, 3M, Minnesota). Reagent inlets were sealed with pressure-sensitive adhesive (9795R, 3M, Minnesota).

Four mechanical slots enabled secure mounting in the automated analyzer.

Portable analyzer and mobile application

The portable analyzer (250 × 170 × 171 mm^3) integrates motion control, magnetic manipulation, thermal regulation, optical detection, and system control modules (Fig. 1c–d). Chip positioning was controlled by two orthogonally arranged stepper motors (T20L, UMot Technology, Chongqing, China) with photoelectric sensors (PM-L25, Panasonic, Osaka, Japan) providing positional feedback. Magnetic bead manipulation employed a stationary magnet (N52D8×10, Dongyang Yixin Magnetic, Jinhua, China) for bead capture and transfer, an ultrasonic transducer (Hainertec, China) for bead dispersion, and an annular magnet array composed of individual magnets (each 5 mm in diameter) for bead redistribution into multiple clusters. Temperature control was achieved using a polyimide heating film coupled to an aluminum heating block with silicone thermal adhesive. A PT1000 thermistor provided real-time temperature feedback (Supplementary Fig. S2). Optical detection was performed using a six-channel fluorescence module, each channel comprising an LED excitation source, optical filters, lenses, and a silicon photodetector. Fluorescence uniformity across channels was validated experimentally (Supplementary Fig. S3). System operation was managed by a microcontroller (STM32F103CBT6) on a custom PCB. An onboard OLED display and Bluetooth module enabled user interaction and wireless communication with a custom Android application. The mobile application supported assay setup, real-time monitoring of amplification curves, automated result interpretation, and data storage (Supplementary Fig. S4).

Chip assembly

Chip assembly followed the workflow shown in Supplementary Fig. S5. First, 30 μL of species-specific RPA reagents was dispensed into each reaction chamber, followed by 7 μL of molten wax (48 °C). The chip was centrifuged at 3000 rpm for 5 min to form a uniform wax barrier. After solidification, 20 μL of elution buffer and 20 μL of silicone oil were sequentially added above the wax layer. The chip was then sealed with the PMMA lid. Washing buffer (1 mL) was loaded into the washing zone, and silicone oil was injected into the transfer zone. Finally, 500 μL of lysis buffer, 20 μL of magnetic beads, 20 μL of proteinase K, and the meat sample were added to the lysis zone. After sealing, the assembled chip was inverted and mounted in the analyzer for automated operation.

Benchtop nucleic acid extraction and reference assays

For comparison, nucleic acids were extracted manually using a standard magnetic bead protocol. Meat samples (up to 1000 mg or 1000 μL homogenate) were mixed with lysis buffer, magnetic beads, and proteinase K, incubated for 5–10 min, washed repeatedly, and eluted in 30 μL of elution buffer. qPCR was performed in 20 μL reactions using PerfectStart® II Probe qPCR SuperMix, with cycling conditions of 94 °C for 30 s followed by 40 cycles of 94 °C for 5 s and 60 °C for 30 s. RPA reactions were performed at 40 °C for 20 min, with fluorescence monitored using a real-time PCR instrument (Beijing Biowe Technology, Beijing, China).

Sample preparation

Fresh sheep, pork, chicken, and duck meat samples were purchased from a certified supermarket. Species purity was confirmed by qPCR following genomic DNA extraction. Liquid homogenates were prepared by mechanical homogenization in phosphate-buffered saline, followed by debris removal. The DNA concentration in each homogenate was precisely quantified using a digital PCR system (Target-One, Beijing, China). These quantified homogenates were used for all optimization and sensitivity validation experiments. For simulated adulteration studies, sheep meat was mixed with duck meat at defined weight ratios using a mechanical grinder. Mixed samples were processed following the same extraction and analysis procedures.

Acknowledgements

This work was financially supported by the National Natural Science Foundation of China (62301537), the Beijing Science and Technology Planning Project (L244090, L248093).

Author details

[1]State Key Laboratory of Transducer Technology, Aerospace Information Research Institute, Chinese Academy of Sciences, Beijing 100190, China. [2]School of Electronic, Electrical and Communication Engineering, University of Chinese Academy of Sciences, Beijing 100049, China. [3]School of Future Technology, University of Chinese Academy of Sciences, Beijing 100049, China

Data availability

The data that support the results of this study are available within the paper and its supplementary information files. Any other relevant data are available from the corresponding author upon reasonable request.

Conflict of interest

The authors declare no competing interests.

Supplementary information The online version contains supplementary material available at https://doi.org/10.1038/s41378-026-01281-6.

Received: 13 January 2026 Revised: 7 February 2026 Accepted: 28 February 2026
Published online: 22 April 2026

References

1. Barnett, J. et al. Consumers' confidence, reflections and response strategies following the horsemeat incident. *Food Control* **59**, 721–730 (2016).
2. Brooks, S., Elliott, C. T., Spence, M., Walsh, C. & Dean, M. Four years post-horsegate: an update of measures and actions put in place following the horsemeat incident of 2013. *NPJ Sci. Food* **1**, 5 (2017).

3. Zhang, W. & Xue, J. Economically motivated food fraud and adulteration in China: an analysis based on 1553 media reports. *Food Control* **67**, 192–198 (2016).
4. Li, X. et al. Meat food fraud risk in Chinese markets 2012–2021. *NPJ Sci. Food* **7**, 12 (2023).
5. Daher, Z. et al. Meat adulteration in the MENA and GCC regions: a scoping review of risks, detection technologies, and regulatory challenges. *Foods* **14**, 3743 (2025).
6. Momtaz, M., Bubli, S. Y. & Khan, M. S. Mechanisms and health aspects of food adulteration: a comprehensive review. *Foods* **12**, 199 (2023).
7. Zarei, M. Infectious pathogens meet point-of-care diagnostics. *Biosens. Bioelectron.* **106**, 193–203 (2018).
8. Nouri, R. et al. CRISPR-based detection of SARS-CoV-2: a review from sample to result. *Biosens. Bioelectron.* **178**, 113012 (2021).
9. Thai, D. A. & Liu, Y. Nucleic acid amplification tests in digital microfluidics: the promise of next-generation point-of-care diagnostics. *Micros. Nanoeng.* **11**, 155 (2025).
10. Mandli, J., El Fatimi, I., Seddaoui, N. & Amine, A. Enzyme immunoassay (ELISA/immunosensor) for a sensitive detection of pork adulteration in meat. *Food Chem.* **255**, 380–389 (2018).
11. Hendrickson, O. D., Zvereva, E. A., Dzantiev, B. B. & Zherdev, A. V. Sensitive lateral flow immunoassay for the detection of pork additives in raw and cooked meat products. *Food Chem.* **359**, 129927 (2021).
12. Cao, Y. et al. A novel method to detect meat adulteration by recombinase polymerase amplification and SYBR green I. *Food Chem.* **266**, 73–78 (2018).
13. Kang, T., Lu, J., Yu, T., Long, Y. & Liu, G. Advances in nucleic acid amplification techniques (NAATs): COVID-19 point-of-care diagnostics as an example. *Biosens. Bioelectron.* **206**, 114109 (2022).
14. Fu, Q., Tu, Y., Cheng, L., Zhang, L. & Qiu, X. A fully-enclosed prototype 'pen' for rapid detection of SARS-CoV-2 based on RT-RPA with dipstick assay at point-of-care testing. *Sens. Actuators B Chem.* **383**, 133531 (2023).
15. Lin, L. et al. A visual method to detect meat adulteration by recombinase polymerase amplification combined with lateral flow dipstick. *Food Chem.* **354**, 129526 (2021).
16. Wang, Z. et al. A finger-driven disposable micro-platform based on isothermal amplification for the application of multiplexed and point-of-care diagnosis of tuberculosis. *Biosens. Bioelectron.* **195**, 113663 (2022).
17. Zheng, T. et al. Specific lateral flow detection of isothermal nucleic acid amplicons for accurate point-of-care testing. *Biosens. Bioelectron.* **222**, 114989 (2023).
18. Tang, D. et al. Point-of-care analysis for foodborne pathogens in food samples based on a fully enclosed microfluidic chip cartridge. *Lab. Chip* **25**, 3537–3548 (2025).
19. Sun, J. et al. Rotary cylinder based fully integrated microfluidic system for the multiplex molecular diagnosis of respiratory pathogens. *Sens. Actuators B Chem.* **447**, 138820 (2026).
20. Cheng, L., Wang, R., Zou, C. & Yan, J. Automated microfluidic system for rapid, multiplexed nucleic acid extraction and detection of pathogens. *Sens. Actuators B Chem.* **426**, 137008 (2025).
21. Xiao, B. et al. Integrating microneedle DNA extraction to hand-held microfluidic colorimetric LAMP chip system for meat adulteration detection. *Food Chem.* **411**, 135508 (2023).
22. Xiao, B. et al. Toothpick DNA extraction combined with handheld LAMP microfluidic platform for simple and rapid meat authentication. *Food Chem.* **460**, 140659 (2024).
23. Xiang, X. et al. High-throughput identification of meat ingredients in adulterated foods based on centrifugal integrated purification-CRISPR array. *Food Chem.* **443**, 138507 (2024).
24. Ding, W. et al. Multi-throughput POCT technology based on RPA and CRISPR/Cas12a and its application in detection of adulterated meat. *ACS Food Sci. Technol.* **3**, 514–523 (2023).
25. Li, Z. et al. Palm-sized lab-in-a-magnetofluidic tube platform for rapid and sensitive virus detection. *Adv. Sci.* **11**, 2310066 (2024).
26. Chen, F. E. et al. Point-of-care amenable detection of Mycoplasma genitalium and its antibiotic resistance mutations. *ACS Sens* **8**, 1550–1557 (2023).
27. Boegner, D. J., Rzasa, J. R., Benke, E. H. & White, I. M. Saliva-STAT: sample-to-answer saliva test for COVID-19. *Sens. Actuators B Chem.* **421**, 136510 (2024).
28. Zhou, T., Li, N., Chen, D. & Wang, J. Fully integrated shockproof magnetofluidic multiplex nucleic acid testing system for infectious disease detection. *Sens. Actuators B Chem.* **442**, 138139 (2025).